Journal of Molecular Catalysis A: Chemical 413 (2016) 100–106

Contents lists available at ScienceDirect

Journal of Molecular Catalysis A: Chemical

journal homepage: www.elsevier.com/locate/molcata

Catalytic oxidation of 2,4,6-tribromophenol using iron(III) complexes with imidazole, pyrazole, triazine and pyridine ligands

Mami Igarashi[a], Qianqian Zhu[a], Masahide Sasaki[b], Ritsu Kodama[a], Kohki Oda[a], Masami Fukushima[a,*]

[a] Laboratory of Chemical Resources, Hokkaido University, Sapporo 060-6828, Japan
[b] National Institute of Advanced Industrial Science and Technology (AIST), 2-17-2-1 Tsukisamu-Higashi, Toyohira-ku, Sapporo 062-8517, Japan

ARTICLE INFO

Article history:
Received 4 November 2015
Received in revised form
19 December 2015
Accepted 21 December 2015
Available online 28 December 2015

Keywords:
Non-heme
Terpyridine
Catalytic oxidation
2,4,6-Tribromophenol
Humic acid

ABSTRACT

Five types of non-heme iron complexes, coordinated with imidazole, pyrazole, triazine and pyridine ligands, which had been previously synthesized, were used in the following studies. Among these complexes, the *mer*-[$FeCl_3$(terpy)] complex showed the highest catalytic activity for the oxidative degradation of 2,4,6-tribromophenol (TrBP) using $KHSO_5$ as an oxygen donor. The turnover numbers for the degradation and debromination of TrBP in the *mer*-[$FeCl_3$(terpy)]/$KHSO_5$ catalytic system were estimated to be 1890 ± 1 and 4020 ± 216, respectively. The catalytic activity was significantly inhibited at pH 4–7 in the presence of a humic acid, a major component of landfill leachates. However, the percent of TrBP degradation and debromination increased at pH 8. GC/MS analyses showed that a major oxidation product was 2,6-dibromo-*p*-benoquinone (DBQ) and its level decreased with increasing reaction time, suggesting that organic acids (identified by LC/TOF-MS) are formed via the ring-cleavage of DBQ. Mineralization to CO_2 was observed to be 15% as a result of the oxidation for a 3 h period, where TOC values before and after the reaction were measured. Absorption spectra of *mer*-[$FeCl_3$(terpy)] with *m*-chloroperoxybenzoic acids as an oxygen donor in acetonitrile showed that a center metal, Fe, formed a peroxide complex with the oxygen donor.

1. Introduction

2,4,6-Tribromophenol (TrBP) is used in the production of fungicides, wood preservatives [1] and an intermediate in the production of brominated flame retardants (BFRs) [2]. TrBP is eluted from landfills where wastes derived from electrical devices including BFRs are disposed of, and this leads to water pollution [3]. In particular, humic acids (HAs) are present in landfill leachates in the form of dissolved organic matter and interactions with HA can enhance water solubility and inhibit the oxidative degradation of organic pollutants [4,5]. Because TrBP has been reported to have endocrine disrupting effects, the TrBP in landfill leachates must be reduced.

Previous studies suggest that Fe(III)-porphyrins, a model of heme enzymes, can be effective for the oxidative degradation of bromophenols and chlorophenols [6–18]. Among the halogenated phenols, bromophenols are relatively resistant to oxidative degradation and dehalogenation [8]. However, mineralization to CO_2 has been reported in the case of a heterogeneous Fe(III)-porphyrin catalyst, which was introduced into an ionic liquid supported Fe_3O_4 [19]. However, in a homogeneous catalytic system, mineralization is minimal, because of catalyst self-degradation.

On the other hand, non-heme enzymes, such as methane monooxygenase, riske dioxygenase, lipoxygenase and catechol dioxygenase, involve iron as a center metal. These enzymes can be activated by an oxygen donor, and organic substrates are oxidized by active species such as $L^{\bullet+}$-Fe(IV)=O, L-Fe(IV)=O and $HO^{\bullet}$ that are produced in such systems [18]. Stable non-heme iron complexes with tetradentate ligands had been synthesized and applied as catalysts for the selective oxidation of olefins [19–24]. However, there are no reports, regarding the catalytic oxidation of halogenated phenols using non-heme iron complexes. Catechol dioxygenases can oxidize catechol, a phenol derivative, via ring-cleavage [20]. In particulars, Dhanalkshmi et al [25]. reported that iron complexes, when coordinated with tridentate ligands, such as pyridine-2,6-dicarboxylic acid, 2,2′:6,2″-terpyridine (terpy) and 2,6-bis(benzimidazol-2′-yl) pyridine, showed higher activities for the oxidation of catechol. This finding suggests that a non-heme

* Corresponding author. Fax: +81 11 706 6304.
E-mail address: m-fukush@eng.hokudai.ac.jp (M. Fukushima).

http://dx.doi.org/10.1016/j.molcata.2015.12.017
1381-1169/

iron complex with a tridentate ligand might be effective for the oxidation of phenol derivatives.

Five types of non-heme iron complexes with monodentate imidazole, pyrazole and tridentate nitrogen ligands (Fig. 1), which had been previously synthesized and their structures determined by X-ray crystallography [26], were prepared. In the present study, the catalytic activities of the non-heme iron complexes for the oxidative degradation of TrBP and the influence of HA on the oxidation of TrBP were investigated. In addition, to characterize the oxidation products of TrBP produced by the non-heme catalyst, the reaction mixtures and CH_2Cl_2 extracts derived from them were analyzed by LC/TOF-MS and GC/MS, respectively. The detection of the activated species of the non-heme complex by the oxygen donor was examined by observing the visible absorption spectrum.

2. Materials and methods

2.1. Materials

Imidazole (im), 1-methylimidazole (meim) (Wako Pure Chemical Industries), 3-methylpyrazole (mepy), 2,4,6-tris(2-pyridil)-1,3,5-triazine (tptz), terpy and TrBP (Tokyo Chemical Industry) were used without further purification. An iron(III) chloride anhydrate was obtained from Nacalai Tesque. $KHSO_5$ was obtained as a triple salt, $2KHSO_5{\cdot}KHSO_4{\cdot}K_2SO_4$ (Merck). Other reagents were obtained from Wako Pure Chemical Industries and were used without further purification. An HA used in this study was extracted from Shinshinotsu peat soil, as described in a previous report [27]. The elemental compositions of the HA were as follows: C 54.5%, H 5.35%, N 2.17%, S 0.66%, O 35.1%, ash 2.22% [28].

2.2. Synthesis and characterization of non-heme iron complexes

Five types of non-heme iron complexes (Fig. 1) were prepared based on the methods previously reported by Cotton et al [26]. The detailed procedures for their preparation can be found in Supplementary Material (Text SM-1). The FT-IR spectra of the synthesized complexes were measured using an FT/IR 600-type spectrophotometer (Japan Spectroscopic Co., Ltd.). Elemental analyses (C, H, N and Cl) of the complexes were carried out by the Instrumental Analysis Division, Equipment Management Center Creative Research Institution, Hokkaido University (Sapporo, Japan). The Fe contents of the complexes were determined using an inductively coupled plasma-atomic emission spectrophotometer (ICPE9000 type, Shimadzu) after wet digestion with a mixture of HNO_3/HCl and the appropriate dilution with ultra-pure water. Analytical data, product yields, elemental composition and FT-IR spectra for each complex were as follows: *mer-[$FeCl_3$(meim)$_3$]*, yield 13.4%; elemental analysis, observed (calculated), %C 35.03 (35.27), %H 4.27 (4.44), %N 20.44 (20.57), %Cl 26.08 (25.43), %Fe 13.7 (13.38); IR spectrum, ν(C—H) 2952 and 1420 cm^{-1}, ν(C—N) 1108 cm^{-1}; *[$FeCl_2$(im)$_4$]Cl*, yield 53.8%; elemental analysis, observed (calculated), %C 32.04 (35.45), %H 3.66 (3.96), %N 24.80 (20.67), %Cl 24.9 (35.45), %Fe 13.0 (11.80); IR spectrum, ν(C—H) 3050 cm^{-1}, ν(C—N) 1261 and 1055 cm^{-1}; *[$FeCl_2$(mepy)$_4$]Cl*, yield 7.48%; elemental analysis, observed (calculated), %C 38.90 (39.16), %H 4.78 (4.93), %N 22.79 (22.84), %Cl 21.84 (21.72), %Fe 11.40 (11.45); IR spectrum, ν(C—H) 2964 and 1442 cm^{-1}, ν(C—N) 1103 and 1049 cm^{-1}; *mer-[$FeCl_3$(tptz)]*, yield 75.7%; elemental analysis, observed (calculated), %C 43.51 (43.10), %H 2.97 (2.79), %N 16.94 (16.51), %Cl 21.04 (21.03), %Fe 11.00 (11.45); IR spectrum, ν(C—H) 1523 and 1468 cm^{-1}, ν(C=C, C=N) 1523 and 1468 cm^{-1}; *mer-[$FeCl_3$(terpy)]*, yield 71.8%; elemental analysis, observed (calculated), %C 45.50 (45.6), %H 2.77 (2.81), %N 10.61 (10.63), %Cl 26.78 (26.93), %Fe 13.70 (13.40); IR spectrum, ν(C—H) 3047 and 767 cm^{-1}, ν(C=C, C=N) 1610, 1468 and 1453 cm^{-1}.

2.3. Assay for TrBP degradation

A 10-mL aliquot of 0.02 M NaH_2PO_4/Na_2HPO_4 buffer (pH 4–8) was placed in a 50-mL Erlenmeyer flask and a 50 μL aliquot of 0.01 M TrBP in acetonitrile was then added to the solution. Aqueous catalysts were added to be produced concentrations of 0.1–10 μM, and a 0.1 mL aliquot of 0.1 M $KHSO_5$ or H_2O_2 was then added to the mixture to start the reaction. After shaking for 30 min, a 1 mL aliquot of the reaction mixture was placed in a glass vial, and 0.5 mL 2-propanol was then added. A 20 μL aliquot of the mixture was injected into a PU980-type HPLC pumping system (JASCO) to analyze the remaining TrBP in the reaction mixtures. The mobile phase was a mixture of methanol and water (78:22 in volume), which was acidified with aqueous 0.08% H_3PO_4, and the stationary phase was a COSMOSIL 5C18-AR-II column (4.6 × 250 nm). The flow rate of the eluent, the column temperature and the detection wavelength were set at 1.0 mL min^{-1}, 50 °C and 290 nm, respectively.

The Br^- that is released as a result of the oxidation was analyzed by an ion chromatography (Dionex IC-120 type, Thermo-Fishers) with conductivity detection. The mobile phase was an aqueous solution of 2.7 mM Na_2CO_3/0.3 mM $NaHCO_3$, and the separation column was an IonPacAS12A analytical column (4 × 200 mm, Thermo-Fishers) with an IonPacAG12A guard column (4 × 50 mm). The flow rate and column oven temperature were set at 1.5 mL min^{-1} and 35 °C, respectively. To evaluate the percent mineralization to CO_2, the concentration of total organic carbon (TOC) in the reaction mixture was analyzed before and after the reaction using a TOC-V CSH type analyzer (Shimadzu). In this test, a stock solution of 0.01 M TrBP was prepared using aqueous 0.01 M NaOH.

2.4. Identification of oxidation products by GC/MS

A 30 mL aliquot of a 0.02 M phosphate buffer (pH 7) containing 200 μM TrBP and 2.7 μM catalyst was placed in a 100-mL Erlenmeyer flask. A 300 μL aliquot of 0.1 M $KHSO_5$ was added and the flask subjected to shaking at room temperature for 1 min, 30 min and 24 h. After the reaction period, a 2 mL aliquot of 1 M ascorbic acid and a 0.5 mL aliquot of 1 mM anthracene in hexane and acetone (1:1) as an internal standard (ISTD) were then added. To adjust the pH of the solution to 11–11.5, a 15 mL aliquot of 600 g L^{-1} K_2CO_3 was added, and 5 mL of acetic anhydride was then added dropwise into the mixture to acetylate the phenolic hydroxyl groups in the TrBP and the oxidation products. This solution was then extracted 3 times with 20 mL of CH_2Cl_2. After dehydration of the organic phase with Na_2SO_4 anhydride, the CH_2Cl_2 was removed by flushing with a stream of dry N_2 gas at 35 °C and the resulting residue was redissolved in 300 μL of CH_2Cl_2. A 1 μL aliquot of the solution was injected into a GC-17A/QP5050 type GC/MS (Shimadzu). Separation was accomplished with a 100% methylsiloxane capillary column (0.25 μm thickness, 0.25 mm i.d. × 25m). Temperature gradient: 65 °C (1.5 min); 65–120 °C (35 °C min^{-1}); 120–130 °C (4 °C min^{-1}); 300 °C (10 min).

2.5. Identification of organic acids using LC/TOF-MS

A 0.1 mL aliquot of aqueous 0.1 M $KHSO_5$ was added to an ammonium formate buffer (pH 8), which contained 50 μM TrBP and 10 μM catalyst. After a 30 min reaction period, a 1 mL aliquot of the reaction mixture was pipetted into a glass vial and 0.5 mL methanol was then added. The organic acids in the reaction mixture were identified and using a 1200 type LC/TOF-MS (Agilent). The stationary phase was a ZORBAX Extend-C18 column (2.1 × 100 mm,

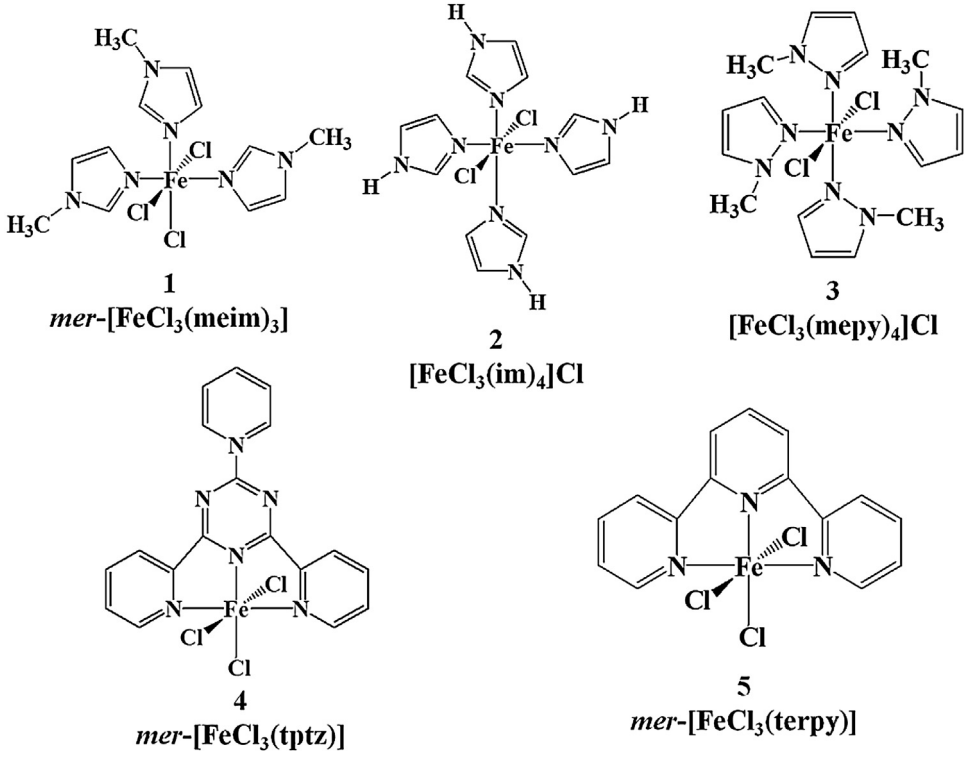

Fig. 1. Structures of the synthesized complexes: *mer*-[$FeCl_3$(*N*-methylimidazole)$_3$] (**1**), [$FeCl_3$(imidazole)$_4$] (**2**), [$FeCl_3$(methylpyrazole)$_4$] (**3**), *mer*-[$FeCl_3$(2,4,6-tris(2-pyridyl)-1,3,5-triazine)] (**4**), *mer*-[$FeCl_3$(terpyridine)](**5**).

1.8 μm particle size, Agilent). The mobile phase was a mixture of acetonitrile/aqueous ammonium formate (10 mM), which was changed from; 1/99 to 80/20 for 35 min and kept 80/20 for 2 min.

2.6. UV–vis absorption spectra

To observe the active species of a non-heme iron complex that was activated by an oxygen donor, 10 μL of 0.1 M *m*-chloroperoxybenzoic acid (*m*CPBA) was added to a 2.5 mL of the acetonitrile solution of 200 μM *mer*-[$FeCl_3$(terpy)] in a quartz cell (1 cm × 1 cm), and UV–vis absorption spectra were recorded at 160 s intervals using a Jasco V-650 iRM type spectrophotometer.

3. Results and discussion

3.1. Catalytic activities for the synthesized complexes

Table 1 shows the percent TrBP degradation for the synthesized complexes using H_2O_2 or $KHSO_5$ as the oxygen donor at pH 7 after a 30 min reaction period. In control cases, no TrBP degradation was observed in the presence of H_2O_2 or $KHSO_5$ alone. For the case of complexes with monodentate ligands *mer*-[$FeCl_3$(meim)$_3$], [$FeCl_2$(mepy)$_3$]Cl and [$FeCl_2$(im)$_4$]Cl, the percent TrBP degradation was less than 10%, while the iron complex with a tridentate ligand, *mer*-[$FeCl_3$(tptz)], indicated 7–8% of degradation. However, approximately 100% of the TrBP was degraded by the *mer*-[$FeCl_3$(terpy)] complex in the presence of $KHSO_5$, although only 5% was degraded when H_2O_2 was used as the oxygen donor. Thus, only the *mer*-[$FeCl_3$(terpy)]/$KHSO_5$ system showed catalytic activity for oxidative degradation of TrBP. The lower activity of the complexes with monodentate ligands, *mer*-[$FeCl_3$(meim)$_3$], [$FeCl_2$(mepy)$_3$]Cl and [$FeCl_2$(im)$_4$]Cl, can be attributed to their instability, compared to the complexes with multidentate ligands. Because the triazine ligand in *mer*-[$FeCl_3$(tptz)] has lower electron donating characteristics, the electron density of the center metal, Fe, would be lower than that in *mer*-[$FeCl_3$(terpy)]. Thus, $KHSO_5$ that can act as an electrophile easily attack to the *mer*-[$FeCl_3$(terpy)]. Zucca et al. [29]. reported a Mn complex with pyridine that had a higher catalytic activity, because of the higher electron density in the center metal. Thus, the catalytic activity of *mer*-[$FeCl_3$(terpy)] was the highest of all the catalysts tested.

Table 1
Influence of catalyst and oxygen donor type on the TrBP degradation. The reaction conditions were as follows: [catalyst] 0.5 μM, [$KHSO_5$] 1 mM, [TrBP] 50 μM, reaction time 30 min and pH 7.

No	Catalysts	Oxygen donor	TrBP degradation (%)
1	*mer*-[$FeCl_3$(meim)$_3$]	H_2O_2	6.61 ± 3.26
		$KHSO_5$	5.51 ± 5.52
2	[$FeCl_2$(im)$_4$]Cl	H_2O_2	7.67 ± 2.68
		$KHSO_5$	9.18 ± 2.30
3	[$FeCl_2$(mepy)$_4$]Cl	H_2O_2	7.07 ± 1.34
		$KHSO_5$	4.40 ± 3.88
4	*mer*-[$FeCl_3$(tptz)]	H_2O_2	8.42 ± 8.42
		$KHSO_5$	7.21 ± 0.30
5	*mer*-[$FeCl_3$(terpy)]	H_2O_2	5.29 ± 0.12
		$KHSO_5$	99.5 ± 0.2

The degradation and debromination kinetics of TrBP by the *mer*-[$FeCl_3$(terpy)]/$KHSO_5$ system were investigated (Fig. SM-1). The percent degradation of TrBP reached 99% within 1 min, and the percent debromination was reached a plateau at approximately 55% when the reaction period was 5 min. Thus, the oxidation of TrBP was too rapid to permit the reaction kinetics in the *mer*-[$FeCl_3$(terpy)]/$KHSO_5$ system to be interpreted. When TrBP and $KHSO_5$ were again added to the reaction mixture after a 30 min period, no degradation of TrBP and/or debromination were observed, suggesting that the *mer*-[$FeCl_3$(terpy)] catalyst had been deactivated. Reiff and Baker, Jr. [30]. reported that terpy ligands might be oxidized in the course of the reaction, e.g., a complex Fe(terpyO_3) with a 2,2′,2″-terpyridine-l, l′,l″-trioxide (terpyO_3) ligand. Thus, the deactivation of the *mer*-[$FeCl_3$(terpy)] catalyst after

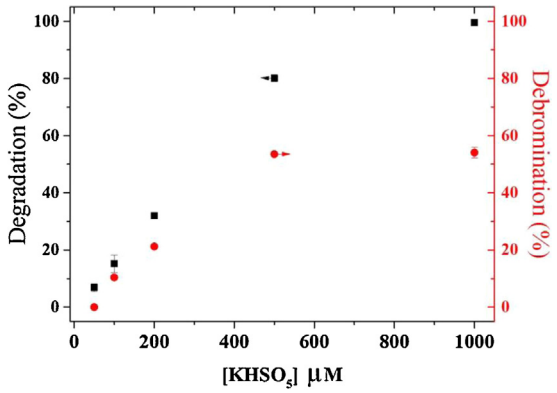

Fig. 2. Influence of $KHSO_5$ concentration on TrBP degradation and debromination. The reaction conditions were as follows: pH 7, [TrBP] 50 μM, [*mer*-[$FeCl_3$(terpy)]] 10 μM, reaction time 30 min.

the first reaction can be attributed to the self-oxidation of the terpy ligand.

Fig. 2 shows the influence of $KHSO_5$ concentration on the percent degradation and debromination of TrBP. The percent degradation and debromination increased with increasing $KHSO_5$ concentration and reached a plateau at concentrations above 500 μM. These results indicate that the *mer*-[$FeCl_3$(terpy)] complex can catalyze the oxidation of TrBP by $KHSO_5$.

Fig. 3 shows the influence of the concentration of *mer*-[$FeCl_3$(terpy)] on the degradation and debromination of TrBP in the presence of 1 mM $KHSO_5$. The percent degradation of TrBP increased linearly with increasing concentration of *mer*-[$FeCl_3$(terpy)]. However, the debromination increased from 0.01 to 0.03 μM of *mer*-[$FeCl_3$(terpy)], while a further addition of the catalyst resulted had no further effect on debromination. The Turnover number (TON) represents one of the indices of catalytic activity and is calculated by dividing the concentration of the degraded TrBP or the Br^- released by the catalyst. At catalyst concentrations of 0.01 μM, the TON values for the degradation and debromination of TrBP were estimated to be 1890 ± 1.4 and 4020 ± 216, respectively.

3.2. Effect of HA on degradation and debromination of TrBP

HAs are a major component of landfill leachates, which contain TrBP. Because HAs can inhibit the oxidation of TrBP in landfill leachates [6,7,19], their influence on the degradation and debromination of TrBP was examined for a variety of pH values (Fig. 4). In the absence of HA, approximately 100% of the TrBP was degraded

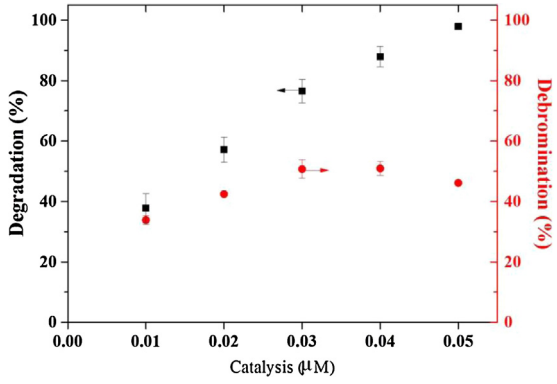

Fig. 3. Influence of *mer*-[$FeCl_3$(terpy)] concentration on the percent TrBP degradation and debromination. The reaction conditions were as follows: pH 7, [TrBP] 50 μM, [$KHSO_5$] 1 mM, reaction time 30 min.

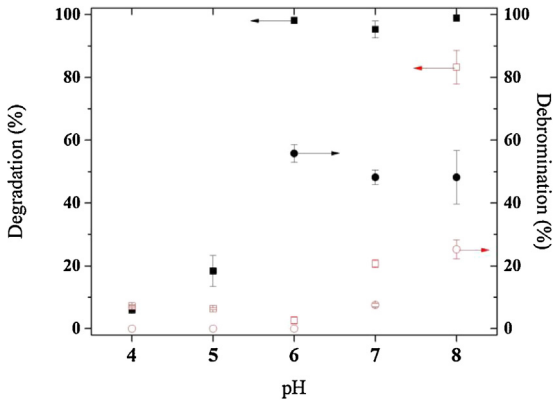

Fig. 4. Influence of pH on TrBP degradation (without HA ■, with HA□) and debromination (without HA ●, with HA ○) in the absence and presence of HA. The reaction conditions were as follows: [TrBP] 50 μM, [*mer*-[$FeCl_3$(terpy)]] 0.5 μM, [$KHSO_5$] 1 mM, reaction time 30 min. [HA] 50 mg L^{-1}.

at pH 6–8 and the percent debromination reached 50%. However, the degradation and debromination of TrBP were remarkably inhibited at pH 4–7, while at pH 8 the percent degradation and debromination increased to 80 and 25%, respectively. In the Fe(III)-ligand (Fe(III)-L)/$KHSO_5$ system, the reactive species produced from Fe(III)-L and $KHSO_5$ ferryl-oxo species (Fe(IV)=O) and/or sulfate radicals ($SO_4^{\bullet -}$) [31–34], that can serve as electrophiles. The pK_a values for TrBP and HA were reported to be 6.31 [35] and 3.5–5.8 [36,37], respectively. Deprotonated species such as phenolate and carboxylate anions for TrBP and HAs can increase the reactivity for electrophiles [38,39]. At pH 4–7, the HAs are largely present as deprotonated species, compared to those for TrBP, because of their pK_a values. Thus, the significant inhibition of the degradation and debromination of TrBP at pH 4–7 in the presence of HA may be attributed to the fact that levels of electron-rich phenolate and carboxylate anions, which is susceptible to attach by an electrophile, are more dominant in HA than in TrBP. The pH values of a typical landfill have been reported to be around 8 [5]. The catalytic system using *mer*-[$FeCl_3$(terpy)]/$KHSO_5$ showed higher degradation and debromination efficiencies at pH 8, and this can be an advantage for degrading bromophenols in landfill leachates.

3.3. Oxidation products

To analyze the byproducts produced as the result of TrBP oxidation by the *mer*-[$FeCl_3$(terpy)]/$KHSO_5$ catalytic system, GC/MS analyses of CH_2Cl_2 extracts of reaction mixtures were conducted after acetylation with acetic anhydride. GC/MS chromatograms after reaction periods of 1 min, 30 min and 24 h are shown in Fig. 5, and the assignments of the reaction products from mass spectra are shown in Fig. 6 (compounds 1–4). The substrate, TrBP (Peak **1** in Fig. 5), was detected in the case of a 1 min reaction period, while 2,6-dibromo-*p*-benzoquinone (DBQ) was detected as a major product (Peak **2** in Fig. 5), and levels of DBQ isomers were also detected (Peaks **3** and **4** in Fig. 5). The levels of DBQ decreased with increasing reaction time, and disappeared after 24 h. However, the formation of dimers, such as phenoxy phenol derivatives, was not detected during the reaction, as reported for the oxidation of 2,4,6-trichlorophenol by an Fe(III)-porphyrin/$KHSO_5$ catalytic system [10]. Thus, it can be expected that the decrease in DBQ in Fig. 5 is due to aromatic ring cleavage, resulting in the formation of organic acids. Thus, an analysis by LC/TOF-MS was conducted to identify the organic acids in the reaction mixture. As shown in Fig. 6, some brominated organic acids are produced. These results suggest that mineralization to CO_2 occurs via ring cleavage. To elucidate this, the TOC in the reaction mixture after 3 h of the reaction

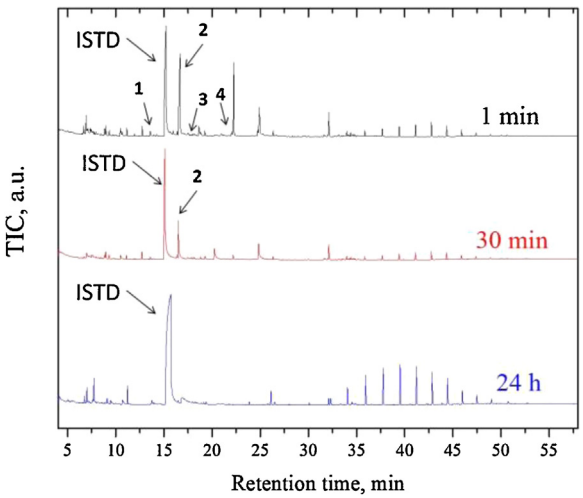

Fig. 5. GC/MS chromatograms of CH_2Cl_2 extracts of reaction mixtures for reaction times of 1 min, 30 min and 24 h. The reaction conditions were as follows: [TrBP] 200 μM, [*mer*-[$FeCl_3$(terpy)]] 2.7 μM, [$KHSO_5$] 1 mM.

period was compared with that before the reaction, and the percent conversion of CO_2 to the degraded TrBP was estimated to be 15%. In the FeTPPS/$KHSO_5$ system, 20% of the degraded pentachlorophenol was mineralized when cyclodextrin was added to the reaction mixture to form the supramolecular catalyst [40], while this is not effective in the case of bromophenol [41]. However, for the case of *mer*-[$FeCl_3$(terpy)], bromophenol was mineralized to CO_2 without the need for any additives, indicating that the *mer*-[$FeCl_3$(terpy)]/$KHSO_5$ catalytic system is effective in the degradation of TrBP.

3.4. *Reactive species from* mer-*[$FeCl_3$(terpy)]*

Radical species, such as $HO^{\bullet}$ or $SO_4^{\bullet-}$ might be generated by the activation of *mer*-[$FeCl_3$(terpy)] with $KHSO_5$, and these species can contribute to the oxidation of organic substrates [41]. Ethanol is generally used as a scavenger of such radical species, as described in the following reactions [43]:

$$HO^{\bullet} + CH_3CH_2OH \rightarrow H_2O + {}^{\bullet}CH(CH_3)OH$$

$$SO_4^{-} + CH_3CH_2OH \rightarrow HSO_4^{-} + {}^{\bullet}CH(CH_3)OH$$

If the above reactions were to be dominant in the presence of ethanol, the percent degradation and debromination of TrBP could be expected to decrease. As shown in Fig. SM-2, the levels of degradation and debromination of TrBP were not changed in the presence of various concentrations of ethanol. These results show that $HO^{\bullet}$ and $SO_4^{\bullet-}$ are not involved in the oxidation of TrBP. In the Fe(III)-porphyrin catalysts, ferryl-oxo species (Fe(IV) = O) are the major reactive species that reproduced as the result of activation with an oxygen donor [31–34,44,45]. Fe(IV) = O species are also detected in non-heme enzymes [46], suggesting that *mer*-[$FeCl_3$(terpy)] may be activated to Fe(IV) = O when $KHSO_5$ is present. In the formation of Fe(IV) = O species, the oxygen donor (X-O-O^{-}) can coordinate with the center metal of the complex (L-Fe(III)) to form a peroxide intermediate (L-Fe(III)-O-O-X), and the OO bond of the L-Fe(III)-O-O-X can be cleaved, as in the pathways below [42]:

$$\text{Homolysis : L-Fe(III)-O-O-X} \rightarrow \text{L-Fe(IV)} = \text{O} + \text{XO}^{\bullet}$$

$$\text{Heterolysis : L-Fe(III)-O-O-X} \rightarrow \text{L}^{\bullet+}\text{-Fe(IV)} = \text{O} + \text{XO}^{-}$$

In the *mer*-[$FeCl_3$(terpy)]/$KHSO_5$ system, $XO^{\bullet}$ (i.e., $SO_4^{\bullet-}$) was found to not participate in the reaction, because the efficiency of degradation of TrBP was not affected in the presence of ethanol, a radical scavenger (Fig. S2). Thus, if L-Fe(III)-O-O-X were formed, the OO bond could be cleaved via heterolysis to form $L^{+\bullet}$-Fe(IV) = O.

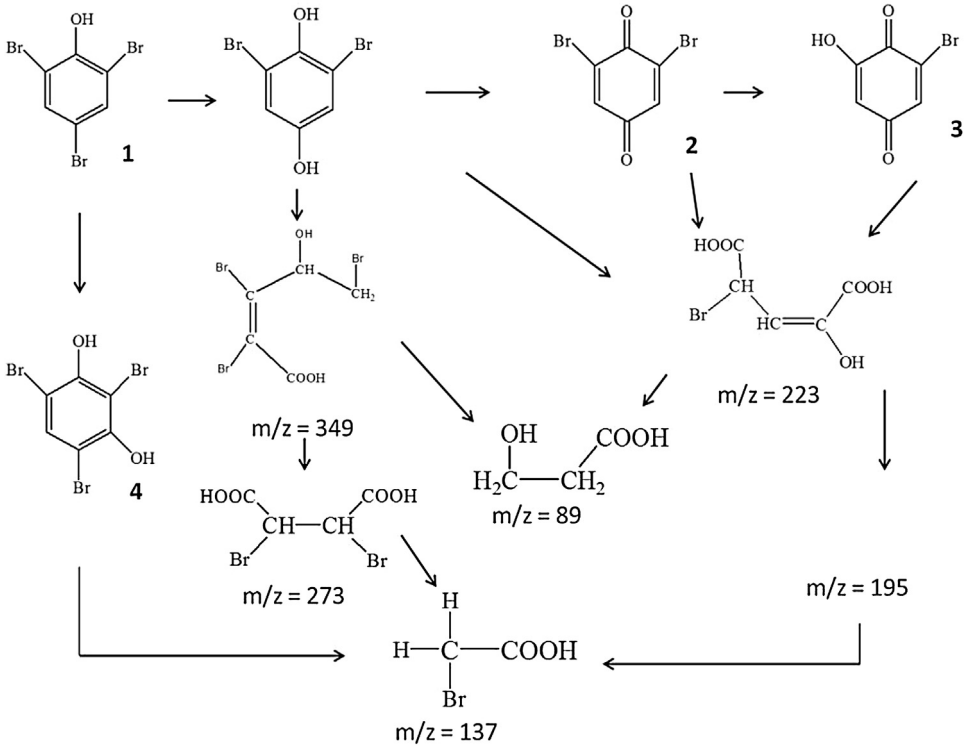

Fig. 6. Organic acids detected by LC/TOF-MS and possible degradation pathways of TrBP by the *mer*-[$FeCl_3$(terpy)]/$KHSO_5$ catalytic system.

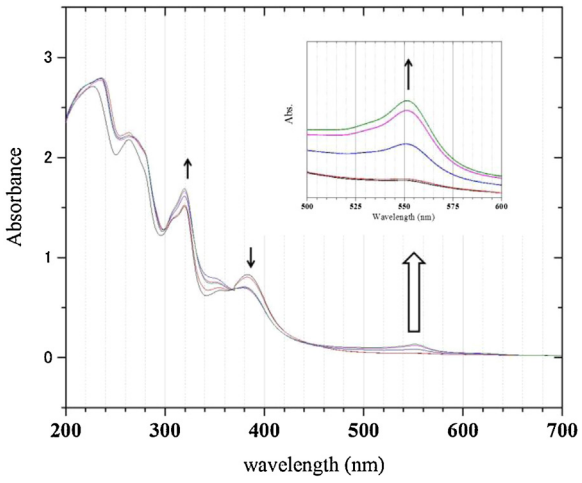

Fig. 7. UV–vis absorption spectra of *mer*-[$FeCl_3$(terpy)] (black line) in CH_3CN and variations in spectra in the presence of *m*CPBA as an oxygen donor. Spectra were recorded at intervals of 160s after adding *m*CPBA. The reaction conditions were as follows: [*mer*-[$FeCl_3$(terpy)]] 200 μM, [*m*CPBA] 400 μM. Insert figure represents the expansion of the spectra from 600 to 500 nm.

Although the direct observation of Fe(IV)=O species is difficult, intermediates derived from L-Fe(III)-O-O-X can be detected in absorption spectra, since they show an absorption maximum at 450–550 nm [47–49]. The *mer*-[$FeCl_3$(terpy)] complex did not absorb in the visible-light region above 460 nm. When absorption spectra were measured with $KHSO_5$ as an oxygen donor, no peaks were observed in the range 450–550 nm. Because $KHSO_5$ is a strong oxidant, the self-degradation of *mer*-[$FeCl_3$(terpy)] can be rapid. The heterolytic cleavage of L-Fe(III)-O-O-X is a polar reaction, with anionic and cationic species being formed. A highly polar solvent such as water can enhance the rate of the reaction, and the intermediates disappear immediately via the self-degradation. Thus, acetonitrile, which a lower polarity than water, and *m*CPBA as the X-O-O^- were employed in our attempts to observe the L-Fe(III)-O-O-X intermediate in absorption spectra. Fig. 7 shows absorption spectra of *mer*-[$FeCl_{3(}$terpy)] in the presence of *m*CPBA. After adding *m*CPBA, the absorption maximum at 551 nm, which can be assigned as (terpy)Cl_2Fe^{III}-O-O-SO_3^-, increased with increasing reaction time, indicating the formation of (terpy)Cl_2Fe^{III}-O-O-SO_3^- [34,35]. These results suggest that the OO bond in the L-Fe^{III}-O-O-SO_3^- cleaves via heterolysis and $L^{\bullet+}$-Fe(IV)=O can act as the active species. The Fe^{IV}=O species for non-heme complexes have been detected using FT-IR spectrometry at −35 °C [50].

6. Conclusion

Catalytic activities of five non-heme complexes (*mer*-[$FeCl_3$(meim)$_3$], [$FeCl_2$(im)$_4$]Cl, [$FeCl_2$(mepy)]Cl, *m*er-[$FeCl_3$(tptz)] and *mer*-[$FeCl_3$(terpy)]), which had been previously synthesized, were evaluated, in terms of the degradation of TrBP in the presence of H_2O_2 or $KHSO_5$ as oxygen donors. The *mer*-[$FeCl_3$(terpy)]/$KHSO_5$ catalytic system showed a higher activity than other catalytic systems. TON values for the degradation and debromination of TrBP by the *mer*-[$FeCl_3$(terpy)]/$KHSO_5$ catalytic system were estimated to be 1890 and 4020, respectively. The major oxidation product was DBQ at the initial stage of the reaction, while its level decreased with increasing reaction time. This can be attributed to the formation of organic acids via the cleavage of aromatic rings, with 15% of the degraded TrBP being mineralized to CO_2. In the oxidation, $KHSO_5$ activates iron(III) to form the peroxy-complex of L-Fe^{III}-O-O-X, suggesting that the reactive species for the degradation of TrBP is $L^{\bullet+}$-Fe^{IV}=O.

Acknowledgment

This work was supported by JSPS KAKENHI Grant Number 25241017.

Appendix A. Supplementary data

Supplementary data associated with this article can be found, in the online version, at http://dx.doi.org/10.1016/j.molcata.2015.12.017.

References

[1] N. Nichkova, M. Germani, M.P. Marco, J. Agric. Food Chem. 56 (2008) 29–34.
[2] C. Thomsen, E. Lundanes, G. Becher, Environ. Sci. Technol. 36 (2002) 1414–1418.
[3] C. Thomsen, E. Lundanes, G.J. Becher, J. Environ. Monit. 3 (2001) 366–370.
[4] K.I. Choi, S.H. Lee, M. Osako, Chemosphere 74 (2009) 460–466.
[5] M. Osako, Y.J. Kim, S. Sakai, Chemosphere 57 (2004) 1571–1579.
[6] Q. Zhu, Y. Mizutani, S. Maeno, M. Fukushima, Molecules 18 (2012) 5360–5372.
[7] Q. Zhu, Y. Mizutani, S. Maeno, R. Nishimoto, T. Miyamoto, M. Fukushima, J. Environ. Sci. Health A 48 (2013) 1593–1601.
[8] M. Fukushima, Y. Mizutani, S. Maeno, Q. Zhu, H. Kuramitz, S. Nagao, Molecules 17 (2012) 48–60.
[9] Q. Zhu, S. Maeno, R. Nishimoto, T. Miyamoto, M. Fukushima, J. Mol. Catal. A-Chem. 385 (2014) 31–37.
[10] M. Fukushima, S. Shigematsu, J. Mol. Catal. A-Chem. 293 (2008) 103–109.
[11] M. Fukushima, J. Mol. Catal. A-Chem. 286 (2008) 47–54.
[12] M. Fukushima, Y. Tanabe, K. Morimoto, K. Tatsumi, Biomacromolecules 8 (2007) 386–391.
[13] M. Fukushima, K. Tatsumi, J. Mol. Catal. A-Chem. 245 (2006) 178–184.
[14] S. Rismayani, M. Fukushima, A. Sawada, H. Ichikawa, K. Tatsumi, J. Mol. Catal. A-Chem. 217 (2004) 13–19.
[15] M. Fukushima, A. Sawada, M. Kawasaki, H. Ichikawa, K. Morimoto, K. Tatsumi, M. Aoyama, Environ. Sci. Technol. 37 (2003) 1031–1036.
[16] M. Fukushima, H. Ichikawa, M. Kawasaki, A. Sawada, K. Morimoto, K. Tatsumi, Environ. Sci. Technol. 37 (2003) 386–394.
[17] T. Miyamoto, Q. Zhu, M. Igarashi, R. Kodama, S. Maeno, M. Fukushima, J. Mol. Catal. B-Enzym. 119 (2015) 64–70.
[18] T. Miyamoto, R. Nishimoto, S. Maeno, Q. Zhu, M. Fukushima, J. Mol. Catal. B-Enzym. 99 (2014) 150–155.
[19] Q. Zhu, S. Maeno, M. Sasaki, T. Miyamoto, M. Fukushima, Appl. Catal. B.-Environ. 163 (2015) 459–466.
[20] M. Abu-Omar, A. Loaiza, N. Hontzeas, Chem. Rev. 105 (2005) 2227–2252.
[21] G. Bilis, K.C. Christoforidis, Y. Deligiannakis, M. Louloudi, Catal. Today 157 (2010) 101–106.
[22] M. Klopstra, G. Roelfes, R. Hage, R.M. Kellog, B.L. Feringa, Eur. J. Inorg. Chem. 4 (2004) 846–856.
[23] Q. Zhang, J.D. Gorden, C.R. Goldsmith, Inorg. Chem. 52 (2013) 13546–13554.
[24] G. Bilis, P. Stathi, A. Mavrogiorgou, Y. Deligiannakis, M. Louloudi, Appl. Catal. A-Gen. 470 (2014) 376–389.
[25] T. Dhanalakshmi, M. Bhuvaneshwari, M. Palaniandavar, J. Inorg. Biochem. 100 (2006) 1527–1534.
[26] S.A. Cotton, V. Franckevicius, J. Fawcett, Polyhedron 21 (2002) 2055–2061.
[27] R.S. Swift, Methods of Soil Analysis, part 3, Soil Science Society of America, Madison, 1996, pp. p1018.
[28] M. Fukushima, S. Tanaka, K. Nakayasu, K. Sasaki, K. Tatsumi, Anal. Sci. 15 (1999) 185–188.
[29] P. Zucca, G. Cocco, S. Maneca, D. Steri, E. Sanjust, J. Mol. Catal. A-Chem. 394 (2014) 129–136.
[30] W.M. Reiff, W.A. Baer Jr., Inorg. Chem. 9 (1970) 570–576.
[31] C. Konstantinos, M. Louloudi, E.R. Milaeva, Y. Deligiannakis, J. Catal. 270 (2010) 153–162.
[32] E.R. Milaeva, O.A. Gerasimova, A.L. Maximov, E.A. Ivanova, E.A. Karachanov, N. Hadjiliadis, M. Louloudi, Catal. Commun. 8 (2007) 2069–2073.
[33] W. Nam, H.J. Han, S.Y. Oh, Y.J. Lee, M.H. Choi, S.Y. Han, C. Kim, S.K. Woo, W. Shin, J. Am. Chem. Soc. 122 (2000) 8677–8684.
[34] C. Perollier, C. Pergrale-Mejean, A.B. Sorokin, New J. Chem. 29 (2005) 1400–1403.
[35] J. Eriksson, S. Rahm, N. Green, Å. Bergman, E. Jakobsson, Chemosphere 54 (2004) 117–126.
[36] M. Fukushima, S. Tanaka, K. Hasebe, M. Taga, H. Nakamura, Anal. Chim. Acta 302 (1995) 365–373.
[37] M. Fukushima, S. Tanaka, H. Nakamura, S. Ito, Talanta 43 (1996) 383–390.
[38] A.T. Stone, Environ. Sci. Technol. 21 (1987) 979–988.
[39] D. Hatzipanayioti, G. Tzeferakos, P. Petropouleas, Chem. Phys. 345 (2008) 119–129.
[40] M. Fukushima, K. Tatsumi, Environ. Sci. Technol. 39 (2005) 9337–9342.
[41] T. Miyamoto, S. Maeno, Q. Zhu, M. Fukushima, J. Mol. Catal. B-Enzym. 110 (2014) 147–153.
[42] S. Maeno, Q. Zhu, M. Sasaki, T. Miyamoto, M. Fukushima, J. Mol. Catal. A-Chem. 400 (2015) 56–63.

[43] G.D. Fang, D.D. Dionysiou, S.R. Al-Abed, D.M. Zhou, Appl. Catal. B-Environ. 129 (2013) 325–332.
[44] K.C. Christoforidis, M. Louloudi, E.R. Milaeva, Y. Deligiannakis, J. Catal. 270 (2010) 153–162.
[45] K. Yamaguchi, Y. Watanabe, I. Morishima, J. Am. Chem. Soc. 115 (1993) 4058–4065.
[46] R.A. Leising, B.A. Brennan, L. Que, J. Am. Chem. Soc. 113 (1991) 3988–3990.
[47] G. Bilis, P. Stathi, A. Mavrogiorgou, Y. Deligiannakis, L. Louloudi, Appl. Catal. A-Gen. 470 (2014) 376–389.
[48] K.B. Jensen, C.J. McKenzie, L.P. Nielsen, J.Z. Pedersen, H.M. Sevendsen, Chem. Commun. (1999) 1313–1314.
[49] F.G. Gelalcha, G. Anilkumar, M.K. Tse, A. Brückner, M. Beller, Chem. Eur. J. 14 (2008) 7687–7698.
[50] J.P. Bigi, W.H. Harman, B. Lassall-Kaiser, D.M. Robles, T.A. Stich, J. Yano, R.D. Britt, C.J. Chang, J. Am. Chem. Soc. 134 (2012) 1536–1542.